Eya4-deficient mice are a model for heritable otitis media

Frederic F.S. Depreux,[1] Keith Darrow,[2] David A. Conner,[1] Roland D. Eavey,[3,4] M. Charles Liberman,[2] Christine E. Seidman,[1,5] and J.G. Seidman[1]

[1]Department of Genetics, Harvard Medical School, Boston, Massachusetts, USA. [2]Eaton-Peabody Laboratory and [3]Pediatric Otolaryngology Service, Department of Otolaryngology, Massachusetts Eye and Ear Infirmary, Boston, Massachusetts, USA. [4]Department of Otology and Laryngology, Harvard Medical School, Boston, Massachusetts, USA. [5]Howard Hughes Medical Institute, Boston, Massachusetts, USA.

Otitis media is an extremely common pediatric inflammation of the middle ear that often causes pain and diminishes hearing. Vulnerability to otitis media is due to eustachian tube dysfunction as well as other poorly understood factors, including genetic susceptibility. As *EYA4* mutations cause sensorineural hearing loss in humans, we produced and characterized *Eya4*-deficient (*Eya4*$^{-/-}$) mice, which had severe hearing deficits. In addition, all *Eya4*$^{-/-}$ mice developed otitis media with effusion. Anatomic studies revealed abnormal middle ear cavity and eustachian tube dysmorphology; thus, *Eya4* regulation is critical for the development and function of these structures. We suggest that some human otitis media susceptibility reflects underlying genetic predisposition in genes like *EYA4* that regulate middle ear and eustachian tube anatomy.

Introduction

Otitis media, an inflammation of the middle ear, accounts for 24 million pediatric office visits annually (1), is responsible for over $4 billion in annual health care costs, and prompts more antibiotic prescriptions and surgery (ear ventilation tubes) than any other pediatric disease (2). Otitis media occurs at least once in 90% of children before age 2 years (3, 4). This extensive vulnerability during childhood reflects immature eustachian tube function (5) as well as other poorly understood susceptibility factors, including environmental triggers and genetic influence (6, 7). Additional etiologies include developmental abnormalities (cleft palate) and nasopharyngeal tumors, conditions that further indicate eustachian tube dysfunction as a primal trigger for otitis media.

Composed of a bony ostium from the middle ear and a distensible cartilaginous segment that links the tympanic cavity to the nasopharynx, the eustachian tube is responsible for regulating middle ear air pressure, removing normal ear secretions, and protecting otic tissues from nasopharyngeal secretions. A highly specialized mucociliary epithelium that lines the tube further supports these physiologic functions. Without normal venting and clearance of secretions by the eustachian tube, mucosal secretions accumulate and the tympanic cavity becomes inflamed and often develops an effusion, features that define otitis media. Otoscopic examination reveals a hypervascular and retracted tympanic membrane. Without an associated infection, pain is minimal, but with microbial invasion, acute otitis media ensues with inflammation, increased middle ear pressure, and resultant outward bulging of the tympanic membrane, producing severe otalgia. Otitis media produces a 25- to 30-decibel (dB) conductive hearing loss that typically reverses when the eustachian tube regains function and the accumulated middle ear fluids are drained. Recognition and treatment of otitis media, with or without infection, may prevent long-term sequelae of hearing loss; speech, language, and learning deficits; and behavioral issues (4).

Human mutations in 2 *EYA* gene family members cause sensorineural hearing loss. Human *EYA1* mutations cause branchiootorenal (BOR) syndrome (OMIM 113650) (8), with branchial arch defects including lacrimal duct abnormalities, preauricular fistulae, and hearing loss (mixed conductive and sensorineural), with abnormally shaped external ears, cochlear malformations, and renal anomalies (9). *EYA4* mutations cause sensorineural hearing loss (DFNA10 locus on chromosome 6) without affecting external ear or other craniofacial structures; these mutations are sometimes accompanied by cardiomyopathy (10–13). The onset of hearing loss due to *EYA4* mutations is notably broad, ranging from early in childhood to adulthood (14), and hearing deficits are not stable until adulthood. Factors accounting for the range of age at onset of hearing loss among identical mutation carriers are unknown.

Eya genes encode transcriptional coactivators (15, 16) that translocate into the nucleus in association with Six molecules, where they regulate gene expression. Functional studies indicate that Eya1 is a nuclear phosphatase that promotes release of transcriptional repression by *Dachshund* on target promoters (17–19). Although genes regulated by Eya molecules remain largely unknown (20), the consequences of human *EYA* mutations implicate these nuclear phosphatases in diverse mammalian organ functions.

To elucidate the roles of *Eya4* in auditory function, we generated *Eya4*-deficient (*Eya4*$^{-/-}$) mice. *Eya4*$^{-/-}$ mice exhibited early-onset and profound hearing defects. In characterizing the mechanisms for deafness in *Eya4*$^{-/-}$ mice, we uncovered otitis media with effusion that occurs in the context of developmental defects in eustachian tube and middle ear. We suggest that *Eya4*$^{-/-}$ mice model human otitis media that arises from eustachian tube dysfunction and illuminate a requirement for this nuclear phosphatase in middle ear maturation. In addition, these data suggest a mechanism to account for variable hearing loss in patients with *EYA4* mutations.

Nonstandard abbreviations used: ABR, auditory brain stem response; dB, decibel; DPOAE, distortion product otoacoustic emission; moET, eustachian tube medial osseous segment; Neo, neomycin; OpTC, eustachian tube opening within tympanic cavity; Zeo, Zeocin.

Conflict of interest: The authors have declared that no conflict of interest exists.

Citation for this article: *J. Clin. Invest.* **118**:651–658 (2008). doi:10.1172/JCI32899.

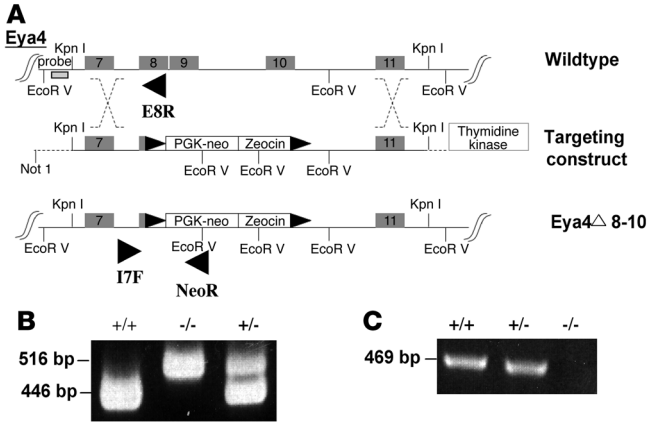

Figure 1

Eya4-targeting strategy. (**A**) A Neo and Zeo cassette flanked by loxP sites (black triangles) was inserted into *Eya4* exons 8–10 by homologous recombination in bacteria. The mutant allele was introduced into ES cells using standard homologous recombination techniques (see Methods). (**B**) PCR analyses of wild-type (+/+), homozygous $Eya4^{-/-}$ (–/–), and heterozygous $Eya4^{+/-}$ (+/–) genotypes. Primers intron 7F (I7F), exon 8R (E8R), and NeoR demonstrated the presence of wild-type (516 bp) and mutant (446 bp) alleles. (**C**) RT-PCR of cardiac cDNA using external forward primer 4F and internal reverse primer 9R identified a single 469-bp product in wild-type (+/+) and heterozygous $Eya4^{+/-}$ (+/–) but not $Eya4^{-/-}$ (–/–) mice.

Results

Production of Eya4-deficient mice. The endogenous *Eya4* gene was targeted by homologous recombination in embryonic stem cells, and heterozygous 129S6/SvEv $Eya4^{+/-}$ mice were produced (Figure 1, A and B, and data not shown). $Eya4^{+/-}$ mice were viable and fertile, but homozygous 129S6/SvEv *Eya4*-null mice ($Eya4^{-/-}$), generated by breeding, died shortly after birth. At weaning, 0 of 337 mice from $Eya4^{+/-}$ matings were $Eya4^{-/-}$ ($P = 6.0E^{-26}$; Supplemental Table 1; supplemental material available online with this article; doi:10.1172/JCI32899DS1). RT-PCR analyses confirmed the absence of *Eya4* RNA in $Eya4^{-/-}$ mice (Figure 1C).

Because of the recognized common occurrence of middle ear infections in the 129S6/SvEv strain (21), $Eya4^{+/-}$ mice were bred onto the CBA/J background. An inbred line was established and characterized and is reported on here. Fortuitously, from the F3 generation onward, most $Eya4^{-/-}$ mice in the CBA/J background survived (Supplemental Table 1), although overall viability of $Eya4^{-/-}$ mice was significantly reduced in comparison with heterozygous mutant or wild-type mice ($P = 1.3E^{-3}$). At birth, body weights of $Eya4^{-/-}$ mice were comparable to wild-type or $Eya4^{+/-}$ littermates. However, adult $Eya4^{-/-}$ mice weighed 25% less than either wild-type or $Eya4^{+/-}$ mice, and at 10 months of age, the average weights of $Eya4^{-/-}$ mice (30.7 ± 4.49 g; $n = 30$) mice were significantly less ($P < 1.0E^{-6}$) than of wild-type (41.2 ± 7.96 g; $n = 25$) or $Eya4^{+/-}$ (40.3 ± 5.23 g; $n = 19$) mice. $Eya4^{-/-}$ females reproduced normally, but male $Eya4^{-/-}$ mice were sterile or had significantly diminished fertility (e.g., only 2 litters were obtained from 13 male $Eya4^{-/-}$ mice of reproductive age; $P < 9.0E^{-14}$) in comparison with normal fertility of heterozygous $Eya4^{+/-}$ male mice.

Hearing deficiency and otitis media in $Eya4^{-/-}$ mice. Because the activities and responses to auditory stimuli by $Eya4^{-/-}$ mice suggested hearing deficits, distortion product otoacoustic emission (DPOAE) and auditory brain stem response (ABR) thresholds were assessed in 10-week-old mice. In comparison with wild-type mice, DPOAE and ABR studies ($n = 4$ each genotype) indicated significant functional loss in peripheral auditory sensitivity of $Eya4^{-/-}$ mice (DPOAE, $P = 4.05E^{-12}$; ABR, $P = 8.66E^{-13}$).

To assess potential mechanisms for hearing loss in $Eya4^{-/-}$ mice, we examined the anatomy and histology of auditory canals (Table 1). Unexpectedly, all 21-day-old $Eya4^{-/-}$ mice ($n = 50$) showed hypervascularity of the tympanic membrane along the manubrium of malleus, marked tympanic membrane retraction, and middle ear effusions (Figure 2A), consistent with otitis media. Tympanic cavities of age-matched wild-type or $Eya4^{+/-}$ mice ($n = 50$; $P = 6.2E^{-18}$) showed no signs of otitis media (data not shown). Examinations of other regional organ systems potentially involved in otitis media, including the respiratory tract, oral cavity, and the eye showed no overt inflammatory or infectious processes in more than fifty 10-week-old $Eya4^{-/-}$ mice.

To exclude the possibility that CBA/J background genes accounted for otitis media with effusion, we bred the $Eya4^{-/-}$ allele onto BALB/c, C57BL/6, and Swiss-Webster backgrounds. *Eya4*-null mice on the BALB/c ($n = 3$), C57BL/6 ($n = 8$), and SW ($n = 3$) backgrounds developed bilateral otitis media with effusion that was indistinguishable from that observed in the CBA/J background (data not shown). Based on the phenotypes of these *Eya4*-null mice, we concluded that background genetic loci (21, 22) were unrelated to observed ear pathology; instead, otitis media with effusion was a direct consequence of *Eya4*-deficiency.

Onset of otitis media. Because the mouse ear undergoes considerable postnatal maturation, we serially characterized ear develop-

Table 1

Evidence of otitis media in $Eya4^{-/-}$ mice with and without antibiotic prophylaxis

	Untreated				Plus azithromycin
Time (d)	0–6	11–12	14–16	21[A]	21
Number of ears	12	6	10	100	14
Tympanic membrane hypervascularity	0	0	10	100[B]	12
Tympanic membrane retraction	N/A[C]	N/A[C]	4	100	12
Middle ear effusion[D] (+bubbles)[E]	0	6	10 (4)	100 (100)	12 (12)

Tympanic membrane hypervascularity and retraction were scored by external examination using qualitative scales. [A]Tympanic membrane hypervascularity and retraction, middle ear fluid, or effusions were absent in 100 ears from age-matched wild-type and heterozygous $Eya4^{+/-}$ mice at age 21 days. $P = 2E^{-29}$. [B]Middle ear inflammation was confirmed by histology in five 21-day-old mice. [C]Tympanic membrane retraction was not assessed in mice fewer than 14 days old. [D]Middle ear fluid was examined in 11- to 12-day-old mice by histology and in older mice (≥14 days) by external examination. [E]Number of ears with bubbles.

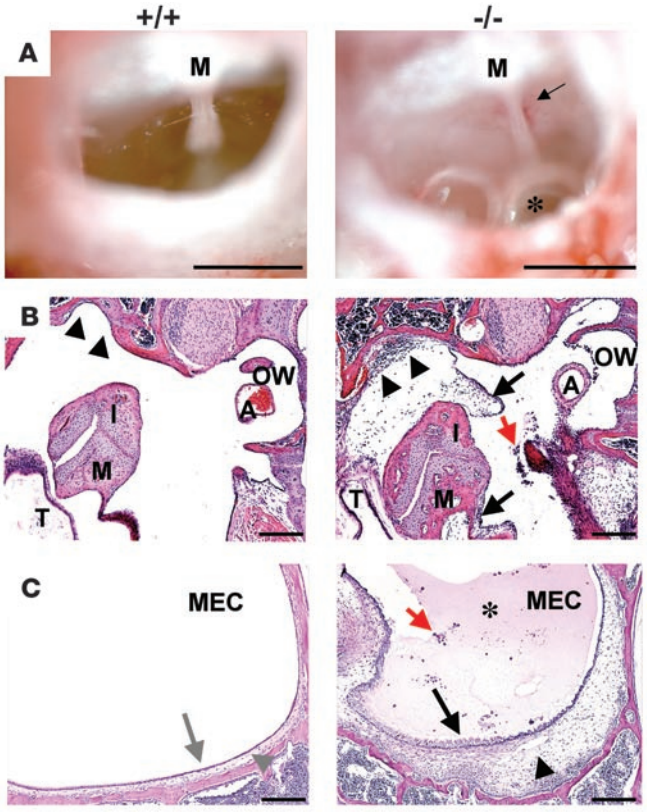

Figure 2
Middle ear pathology in *Eya4*$^{-/-}$ mice. (**A**) Macroscopic views of tympanic membrane from wild-type (+/+) and *Eya4*$^{-/-}$ (–/–) mice. *Eya4*$^{-/-}$ mouse ears had air bubbles (asterisk), indicative of middle ear effusion, and dilated capillaries (black arrow) as well as tympanic membrane retraction (see also Figure 3). Scale bars: 1 mm. (**B** and **C**) PAS-stained paraffin sections of mice, age 3 weeks. (**B**) The mesotympanum of middle ear cavity shows inflammatory cells (red arrow) in *Eya4*$^{-/-}$ mice, and the mucoperiosteum (black arrowheads) is thickened. A, stapedial artery; I, incus; M, malleus; OW, bony niche of the oval window; T, tympanic membrane. Scale bars: 200 μm. (**C**) The hypotympanum regions of *Eya4*$^{-/-}$ mice show effusion (asterisk), inflammatory cells (red arrow), hyperplastic ciliated epithelial cells (black arrows), and expanded lamina propria connective tissue in the mucoperiosteum (arrowhead; corresponding regions denoted by gray arrow/arrowhead in wild-type). MEC, middle ear cavity.

ment in wild-type and *Eya4*$^{-/-}$ mice (Table 1) to date the onset of otitis media. Before day 6, the external earflap (pinna) was folded in both wild-type and *Eya4*$^{-/-}$ mice, providing a protective barrier, and the middle ear cavity was filled with mesenchymal cells, as has been previously reported (23). There was no delay in the onset of middle ear cavitation (24), which became evident at day 6, and no inflammation in the newly formed small middle ear space in wild-type or *Eya4*$^{-/-}$ mice (Figure 3A). At days 11–12, when the pinna was unfolded in all mice, the middle ear cavity was largely aerated and mesenchymal cells were found only near ossicles in wild-type mice. In contrast, the middle ear cavity of *Eya4*$^{-/-}$ mice remained full of mesenchyme but showed no signs of inflammation (Figure 3B).

By postnatal days 14–16, tympanic membrane retraction and middle ear effusions, with or without air bubbles, were seen through the eardrum of *Eya4*$^{-/-}$ mice (Figure 3C) and the middle ear mucosa showed inflammation in all mutant ears (n = 10; Table 1). At weaning (day 21), all *Eya4*$^{-/-}$ mice, but no wild-type mice, had tympanic membrane retraction with hypervascularity and middle ear effusion with or without air bubbles (Figure 2A and Table 1; *Eya4*$^{-/-}$, n = 50; wild-type, n = 40; $P = 6.2E^{-18}$). Young *Eya4*$^{-/-}$ mice had serous effusions that contained few or no granulocytes (Figure 2, B and C); effusions in older *Eya4*$^{-/-}$ mice were more purulent and contained abundant granulocytes (data not shown).

Antibiotic prophylaxis in Eya4$^{-/-}$ *mice*. To assess whether antibiotics could suppress otitis media and effusions in *Eya4*$^{-/-}$ mice, we administered azithromycin to pregnant females and continued prophylactic antibiotic treatment until pups were weaned. Azithromycin is efficacious in treating a variety of rodent models of human infection, including acute otitis media due to *Haemophilus influenzae* (25). At age 3 weeks, the tympanic cavities from both ears of 39 mice were evaluated for signs of effusion and inflammation (wild-type, n = 13; *Eya4*$^{+/-}$, n = 19; *Eya4*$^{-/-}$, n = 7). Visual inspection suggested no otitis media in 33 mice (all wild type; all *Eya4*$^{+/-}$; 1 *Eya4*$^{-/-}$), and histological studies confirmed the absence of effusion or inflammatory cells (Figure 4A and Table 1). In contrast, 6 of 7 azithromycin-treated *Eya4*$^{-/-}$ mice had tympanic cavities with erythema, dilated capillaries, and histologic sections that demonstrated effusion and inflammation. We interpreted the persistence of otitis media with effusion in azithromycin-treated *Eya4*$^{-/-}$ mice to indicate a predominant nonbacterial etiology.

Eustachian tube dysfunction. Impaired eustachian tube function is recognized as the initial mechanism that triggers otitis media in humans (5). Impairment can be transient, as occurs during an acute upper respiratory tract infection, or can be more permanent, as occurs with tumor obstruction (26) or craniofacial anomalies, such as cleft palate (5). Because *Eya1*-null mice have multiple craniofacial abnormalities, including palatal defects (27), we considered whether similar anatomic defects occurred in *Eya4*$^{-/-}$ mice and increased otitis media susceptibility. Skull preparations of 4-week-old wild-type and *Eya4*$^{-/-}$ mice (n = 3, each genotype) showed no overt craniofacial or palatal defects (Figure 5, A and B; data not shown). However, newborn *Eya4*$^{-/-}$ mouse skulls (n = 8) demonstrated incomplete fusion of palatal bones (Figure 5, C and D); the lack of fusion was not observed in newborn wild-type mice (n = 4; P = 0.002). We concluded that Eya4 deficiency resulted in a developmental delay rather than a fixed defect in skull bone maturation.

To identify other anatomical defects that might contribute to otitis media development, we analyzed the middle ear cavity and eustachian tube of *Eya4*$^{-/-}$ and wild-type mice (n = 4 each genotype) and assembled serial light micrographs into 3D reconstructions. Although the bony capsule of the middle ear was smaller in *Eya4*$^{-/-}$ mice than in wild-type mice, otic structures appeared normal (data not shown). The eustachian tube opening within the tympanic cavity (OpTC) (Figure 4A) is formed by the tube's medial osseous segment (moET). Although eustachian tube length (measured from the ostium along the lateral cartilaginous segment to the torus tubarius of the nasopharynx; Figure 4B) was 3 mm in both wild-type and *Eya4*$^{-/-}$ mice (Table 2), both the moET and OpTC in *Eya4*$^{-/-}$ mice were abnormal and diminutive (Figure 4B and Table 2), approximating only 50% of the moET in wild-type mice. Scanning electron micrographs (n = 5 for each genotype) showed that the OpTC was narrowed and abnormally positioned at the ante-

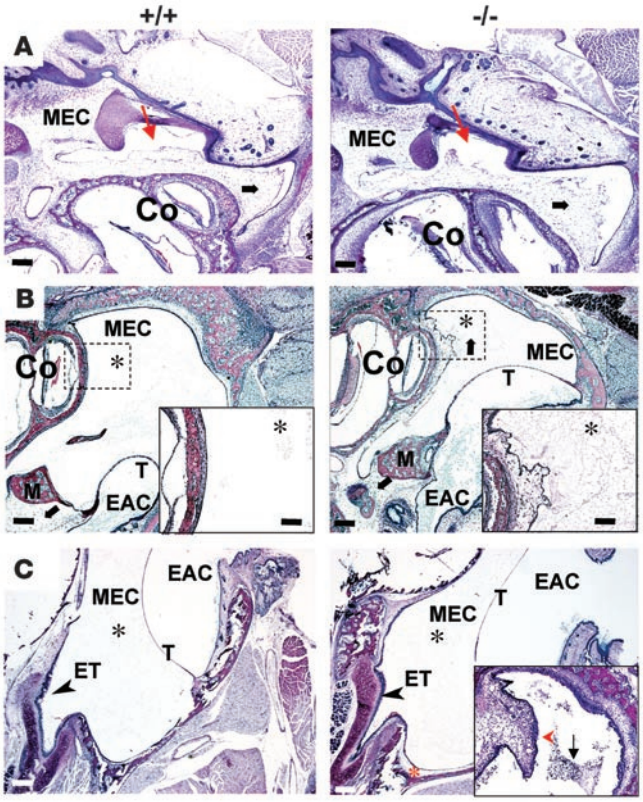

Figure 3
Comparison of postnatal middle ear cavitation in wild-type (+/+) and *Eya4*$^{-/-}$ (–/–) mice. (**A**) Six-day-old mice (n = 6, each genotype) had no middle ear effusions. Mesenchymal cells (black arrows) are found in the middle ear cavity, but the middle ear space (red arrows) is visible. Co, cochlea. Scale bars: 200 μm. (**B**) At days 11 and 12 (n = 3 mice of each genotype), mesenchymal cells (black arrows) have largely disappeared from the middle ear cavity of wild-type mice, but a few cells remain around the ossicles. M, malleus. Many more mesenchymal cells and collagen (asterisks), a by-product of mesenchyme regression, are present in the MECs of *Eya4*$^{-/-}$ mice than in wild-type mice. See magnified inset (scale bars: 200 μm) showing mucoperiosteum and mesenchyme regression. The marked inward bulging of tympanic membrane in *Eya4*$^{-/-}$ mice correlated with tympanic membrane retraction that was visible through the external auditory canal (EAC). Scale bar: 40 μm. (**C**) At days 14–16 (n = 5 for each genotype), some collagen (black asterisks) remains in both genotypes, but *Eya4*$^{-/-}$ mice also show a hyperplastic mucosa (red asterisk) with inflammation. The opening of the eustachian tube (ET) is indicated (arrowheads). Inset shows a polyp (red arrowhead) and numerous inflammatory cells (black arrow) found in some *Eya4*$^{-/-}$ mice.

rior perimeter of the middle ear in *Eya4*$^{-/-}$ mice (Figure 6A). Some (20%) *Eya4*$^{-/-}$ mice had a polyp that obstructed the OpET (Figure 6A). Polyps were absent in ears of all wild-type mice.

Eustachian tube dysmorphology corresponded to developmental expression of *Eya4*. In situ hybridization of E10.5 and E12 embryos (Supplemental Figure 1, A and B) confirmed previously reported *Eya4* expression in the otic vesicle (16) and also revealed expression in the developing semicircular canals and cochlea but not in the nascent endolymphatic duct. We found that *Eya4* expression was also strong in the middle ear–forming region and surrounding the first branchial pouch, from which eustachian tube structures were derived (28).

Middle ear cilia morphology. Cilia within the eustachian tube are critically involved in clearance of normal secretions and abnormal fluids (5), and patients with primary ciliary dyskinesia or Kartagener syndrome have increased incidences of otitis media (29). Because *Eya4* was expressed in eustachian tube mucociliary epithelia of newborn mice (Supplemental Figure 1C), we considered whether ciliary abnormalities contributed to otitis media in *Eya4*$^{-/-}$ mice. Using scanning electron microscopy, we assessed the integrity of the mucociliary epithelium in wild-type and *Eya4*$^{-/-}$ mice (n = 6 each genotype). At weaning, the cilia in mutant and wild-type mice were comparable in number and morphologically indistinguishable (Figure 6B), implying that *Eya4* did not have an essential developmental role for these specialized structures. Despite normal-appearing cilia, the middle ear cavity epithelium of young *Eya4*$^{-/-}$ mice was swollen and had increased numbers of goblet cells compared with wild-type littermates (Figure 6B). At 16 months, the cilia density was diminished in *Eya4*$^{-/-}$ mice (Figure 6C) and epithelial swelling was more pronounced. We interpreted the temporal progression of initially normal numbers and appearance of cilia to progressive epithelial swelling and cilia loss to indicate that otitis media caused rather than resulted from a compromised mucociliary epithelium in *Eya4*$^{-/-}$ mice.

Fbxo11, Six1, and Eya1 expression. Middle ear inflammation and increased otitis media susceptibility have been observed in mice with mutations in *Eya1*, *Six1*, and *Fbxo11* (27, 30–32). To determine whether *Eya4*$^{-/-}$ mice developed otitis media because these genes were dysregulated by the absence of Eya4, we compared expression in wild-

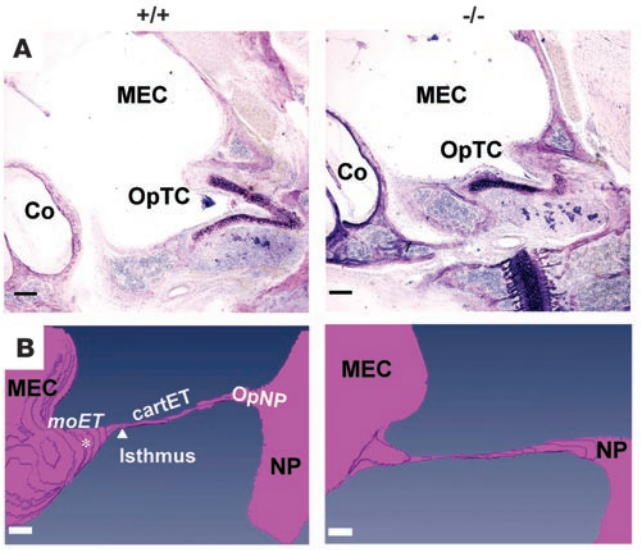

Figure 4
Morphometry of wild-type (+/+) and *Eya4*$^{-/-}$ (–/–) middle ear cavity in azithromycin-treated mice. (**A**) The OpTC of *Eya4*$^{-/-}$ mice was smaller than that in wild-type. Scale bars: 200 μm. (**B**) A 3D reconstruction of portions of the middle ear cavity, eustachian tube, and nasopharynx (NP). The moET, isthmus, cartilaginous segment (cartET), and opening of the eustachian tube within the nasopharynx (OpNP) are indicated on the wild-type 3D reconstruction. The location of the OpTC is denoted (white asterisk). Eustachian tube dimensions (see Table 2) were obtained by measurement of the structures identified. Scale bar: 300 μm.

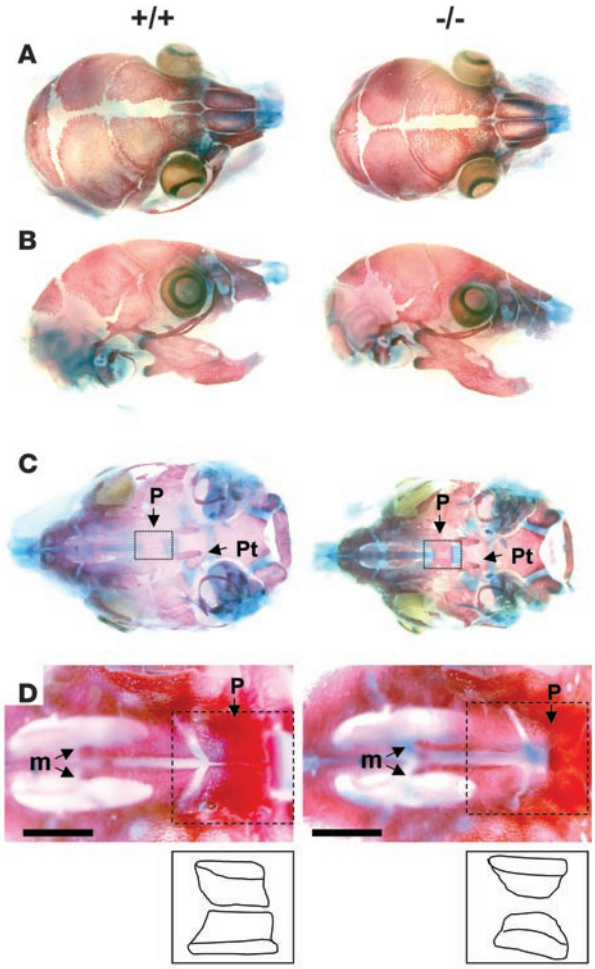

Figure 5
Bone and cartilaginous skull tissue anatomy of wild-type (+/+) and *Eya4*$^{-/-}$ (–/–) newborn mice. Top (**A**) and lateral (**B**) skull views demonstrated no craniofacial abnormalities in mutant or wild-type mice (n = 3 for each genotype), but ventral view (**C**) showed abnormal fusion of palatal bones (dashed box) in *Eya4*$^{-/-}$ mice. (**D**) Higher magnification of palatal bones (**C**, dashed box) and schematic detailing morphologic abnormalities. Note wide separation between flanking palatal bones (incomplete fusion) in *Eya4*$^{-/-}$ skulls. Pt, pterygoid bone; m, maxillary shelves; P, palate bone. Scale bar: 1 mm.

type and mutant mice. At E12.5, *Eya1* and *Six1* expression was comparable in wild-type and *Eya4*$^{-/-}$ mice (Supplemental Figure 2, A–D; n = 3, each genotype). *Fbxo11* expression was studied in the cochlea of newborn *Eya4*$^{-/-}$ pups and also was comparable to that found in wild-type mice (Supplemental Figure 2E; n = 2 each genotype).

Discussion

Heritability studies and familial aggregations suggest an important role for genetics in otitis media susceptibility; however, knowledge of the identity and function of genes that participate in middle ear development and their contribution to otitis media remains lacking. Here, we demonstrate a critical role for *Eya4* in structuring the eustachian tube, particularly the moET, and positioning the opening of the tube within the middle ear. We found that eustachian tube maldevelopment in *Eya4*$^{-/-}$ mice impaired normal tube function and rendered mice profoundly susceptible to otitis media with effusion.

The major physiologic functions of the eustachian tube include ventilation/pressure regulation of the middle ear, protection of the middle ear from nasopharyngeal secretions, and clearance of middle ear secretions via the tube into the nasopharynx (5). Tubal physiology is predicated on appropriately sized and positioned orifices in the middle ear cavity and the nasopharynx in addition to tubal function. In *Eya4*$^{-/-}$ mice, the middle ear cavity was small, the osseous segment of the eustachian tube diminutive, and the middle ear orifice of the tube reduced and malpositioned. In the neonatal period, middle ear cavity size and malformation would impair redistribution of embryonic mesenchyme cells (33), which would account for the prolonged mesenchymal disappearance that occurred in *Eya4*$^{-/-}$ mice. In addition, the developmental delay in palate fusion found in *Eya4*$^{-/-}$ mice might superimpose dysfunction at the nasopharyngeal end of the eustachian tube, as occurs in human palate clefting. Both structural malformations and eustachian tube dysfunction would mechanically impede clearance of normal middle ear secretions in *Eya4*$^{-/-}$ mice and predispose to polyp formation and loss of cilia (Figure 6), as occurs in experimentally induced eustachian tube malfunction (34). Taken together, the primary anatomic defects produced by genetic loss of *Eya4*$^{-/-}$ would so impair ventilation and clearance functions of the eustachian tube that mice become uniformly susceptible to otitis media as manifest by secondary responses (e.g., effusion, polyp formation, and loss of cilia).

Eya4$^{-/-}$ mice demonstrated salient features of human otitis media that is caused by eustachian tube dysfunction, including juvenile onset erythema plus retraction of the tympanic membrane

Table 2
Eustachian tube dimensions of wild-type and *Eya4*$^{-/-}$ mice

Genotype	OpTC length	OpTC diameter	OpTC height	ET length	OpNP length	OpNP diameter
+/+	774 ± 62	866 ± 74	280 ± 33	1738 ± 113	514 ± 102	405 ± 93
–/–	422 ± 64	471 ± 119	130 ± 20	1831 ± 289	555 ± 179	278 ± 154
P value	0.0005	0.005	0.0006	NS	NS	NS

Eustachian tube (ET) measurements (μm) in azithromycin-treated wild-type (+/+) and *Eya4*$^{-/-}$ (–/–) mice (n = 4, each genotype). Six measurements were taken from x and y axes of 3D surfaces of the OpTC, including the following: diameter of the ostium; length, distance from the center of the ostium diameter to the eustachian tube isthmus; height, determined on z axis by the number of sections required to form top of eustachian tube ostium to the first section entering into the isthmus. Along the cartilaginous portion, eustachian tube length was the distance from the isthmus to the starting point of enlargement of eustachian tube into nasopharynx. At the opening of the eustachian tube in the nasopharynx (OpNP), diameter was taken at the torus tubarius, and length was the distance from starting point of enlargement of eustachian tube to the center of torus tubarius diameter. Histological annotations of these definitions are shown in Figure 4. Mean values ± SD are shown. P values are based on comparisons with wild-type.

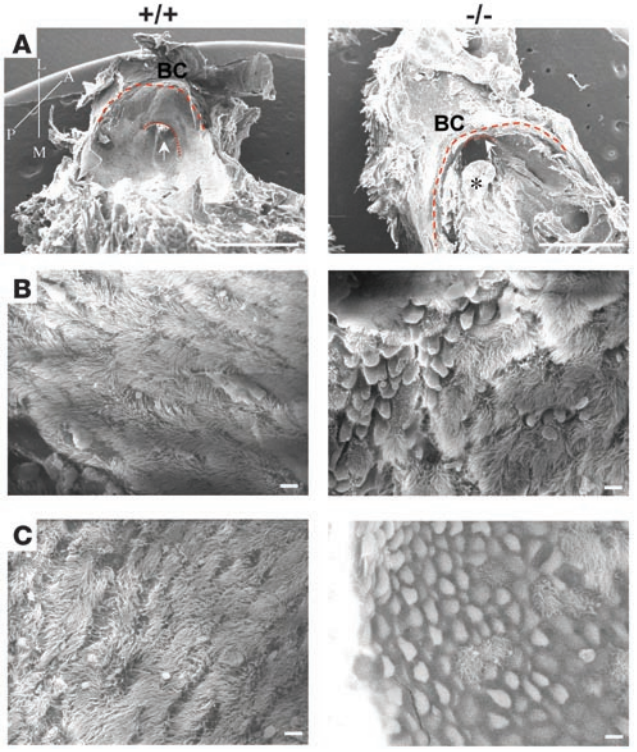

Figure 6
Scanning electron micrographs of middle ear cavities from wild-type (+/+) and *Eya4*$^{-/-}$ (–/–) mice. (**A**) Lateral view of the eustachian tube ostium (arrow) from 16-month-old mice. The ostium is malpositioned in the *Eya4*$^{-/-}$ ear, near to the edge of the middle ear bony capsule (BC). The junction of the bony capsule with the temporal bone (thick dashed line) and the osseous portion of eustachian tube (thin dashed line) are highlighted. A polyp (asterisk) is obstructing the *Eya4*$^{-/-}$ OpTC. Axis: A, anterior; P, posterior; L, lateral; M, medial. Scale bars: 1 mm. (**B**) Lateral view of eustachian tube ostia epithelia in 3-week-old mice shows increased numbers of goblet cells and swollen epithelia in *Eya4*$^{-/-}$ mice, although cilia are morphologically indistinguishable from cilia in wild-type mice. Scale bars: 5 μm. (**C**) The mucociliary epithelia at the eustachian tube ostia of 16-month-old mice show rarefaction of cilia in the mucosa of *Eya4*$^{-/-}$ mice. Scale bars: 5 μm.

and middle ear effusion. The changes observed in the eustachian tube mucociliary epithelium of *Eya4*$^{-/-}$ mice, including diminished cilia density and increased numbers of goblet cells, also typify histopathologic findings of childhood otitis media (35). Based on the restricted developmental defects produced by Eya4 deficiency and the absence of evidence suggesting primary infection (e.g., serous effusions and absence of bacteria on histopathology, lack of overt pain or systemic manifestations, and failure of antibiotic prophylaxis), we suggest that *Eya4*$^{-/-}$ mice provide a new genetic model for pediatric otitis media susceptibility caused by eustachian tube dysfunction. Further insights into *Eya4* targets that influence eustachian tube morphology and physiology may indicate new therapeutic pathways for this prevalent childhood disorder.

Eya4$^{-/-}$ mice expand our knowledge about genetic determinants that protect against otitis media. Increased susceptibility to infectious otitis media has been identified in other mouse strains (21, 22), in mice with spontaneous mutations (36, 37), and in mice that, like *Eya4*$^{-/-}$ mice, were engineered to carry a specific gene mutation (38–40). These mice indicate several distinct mechanisms by which otitis media vulnerability can be increased. A missense mutation in the TLR4 gene renders C3H/HeJ mice unresponsive to LPS and vulnerable to Gram-negative organisms, including *H. influenzae*, one of the common bacterial causes of human otitis media (41). *Evi1*-null mice, produced during a N-ethyl-N-nitrosourea mutagenesis screen, exhibited increased susceptibility to otitis media, possibly by affecting transcriptional regulation of neutrophil or mucin genes through a TGF-β/SMAD signaling pathway (42). Susceptibility to otitis media by *Jeff* mice reflects an *Fbxo11* mutation; this F-box gene may influence ubiquitination pathways and impair inflammatory responses in the middle ear or increase infection because of associated craniofacial abnormalities (including cleft palate) found in *Jeff* mice (31, 32). Both *Eya1*- and *Six1*-deficient mice (27, 30) also have craniofacial anomalies affecting the palate and show increased middle ear inflammation, observations that underscore the importance of Eya/Six transcriptional complexes in middle ear development and function. While our studies found no evidence for direct regulation by Eya4 of Fbox11, Eya1, or Six1, further analyses of these transcriptional networks may reveal crosstalk that links developmental pathways in the middle ear.

An intriguing question raised by these studies is whether otitis media contributes to hearing loss in human patients with dominant *EYA4* mutations. The broad range of age at onset of hearing deficits and the initially progressive but subsequently stable fixed deficit found later in life are atypical for a genetic form of sensorineural deafness. We speculate that some clinical variability in onset of hearing loss among mutation carriers reflects *Eya4*-mediated susceptibility to otitis media with or without infection in addition to dysregulation of *Eya4* targets that directly participate in sensorineural hearing processes.

Methods

The Animal Care and Use Committee of Harvard Medical School approved all procedures involving mice.

Gene targeting. An 11.6-kb NheI genomic fragment encoding *Eya4* exons 7 to 11 was subcloned from a genomic 129S6/SvEv BAC library (Invitrogen) into a vector carrying thymidine kinase selection marker (gift of J. Rossant, Hospital for Sick Children, Toronto, Ontario, Canada). The neomycin (Neo) resistance gene was inserted into *Eya4* sequences using homologous recombination in *Escherichia coli* (43). In brief, a 2481-bp segment encoding Neo and Zeocin (Zeo) resistance genes flanked by LoxP sites was PCR amplified using the following primers: forward, TGCTATTTTTCTGATATTTAGGCCCTATCCACACATTCTTTCTACACCAGCAGCTCAAACggatcctctagagtcgagg; reverse, GAAGAGCTTCCTAACTGCGTCCAATATCAAGTGATCAGCCCTGAAATAATCTATATATCCcccctcgaggacc. These primers share 5′ ends homologous to *Eya4* genomic sequence (upper-case letters) and 3′ ends homologous with plasmid sequences (lower-case letters) carrying a LoxP-Neo/Zeo-LoxP cassette constructed by inserting a Zeo cassette with bacterial promoter 3′ of the Neo cassette. Amplicon and circular thymidine kinase template plasmid were coelectroporated into *E. coli* RecE/RecT YZ2000 competent cells (gift of Francis Stewart, University of Technology, Dresden, Germany). The targeting construct was then electroporated into embryonic stem cell line 129S6/SvEv Tc1 (gift of Philip Leder, Harvard Medical School), and desired clones were identified by Southern blot analyses using a 5′ P^{32}-labeled probe (see Supplemental Figure 1). Recombinant embryonic stem cell clones were injected into mouse blastocysts. PCR-based genotyping of tail DNA was performed using the following primers: forward, intron 7F, GCTGGCCACGACCATTATTCCC;

and reverse, wild-type primer, exon 8R, ACGGCCGGCTGCTGCATC, and Neo primer, NeoR, GCCAAGCTAGCTTGGCTGGACG.

RNA analysis. RNA was extracted from selective tissues using TRIzol reagent (Invitrogen). About 1.5 μg of total RNA and 50 ng of random primer were used for reverse transcription. Primers to assess *Eya4* exon deletions were exon 4F, CGGAACCTCAGAATTCCAGG; and exon 9R, GCTGGCAACATCACACCAAGATCG. A 157-bp *Fbxo11* amplicon was assessed in cochlea RNA using the following primers: forward, TTGGTGCAGCACCTGGCAAGGTTG; and reverse, GTGTGCGTTGTGATGCTGAGCAG.

In situ hybridization. Sense and antisense digoxigenin-labeled probes were transcribed from a linear pCR4Blunt-TOPO (Invitrogen) plasmid carrying *Eya4* exons 8 to 12 cDNA. An 855-bp probe for *Six1* was amplified using the following primers: *Six1*, forward, ATGTCGATGCTGCCGTCGTTTGG; and *Six1*, reverse, TTAGGAACCCAAGTCCACCAAACTGG. A 720-bp probe for *Eya1* was amplified using the following primers: *Eya1*, forward, ATGGAAATGCAGGATCTAACCAGC; and *Eya1*, reverse, CGTCATGTAGTGTGCTGGATAC. Fragments were cloned into pCR4Blunt-TOPO (Invitrogen) plasmid, transcribed as described for *Eya4* probes, and hybridized to either whole mouse E12.5 embryos or to 10-μm paraffin-embedded sections (44).

DPOAE and ABR thresholds. Hearing was studied in anesthetized (intraperitoneal xylazine, 20 mg/kg, and ketamine, 100 mg/kg) 10-week-old CBA/J wild-type and mutant mice (F3 generation). Distortion products at $2f_1$-f_2 were measured for both ears as described previously (45), using primary-tone level with f2/f1 = 1.2, f2 level 10 decibel lower than f1, and primaries in increments of 5 dB. Threshold was defined as the f1 level required to produce a DPOAE at 0 dB sound pressure level. ABR potentials were recorded by insertion of needle electrodes at the vertex, pinna, and tail. Sound levels were increased in 5-dB steps, and responses were amplified, filtered, and averaged using an A-D board in a LabVIEW-driven data acquisition system (National Instruments). ABR thresholds were determined by visual inspection of stacked waveforms and by evaluation of the growth of peak-to-peak response amplitude with increasing sound pressure level (46).

Antibiotic prophylaxis. Azithromycin (50 mg/kg/d) (47) was added to drinking water (final concentration of 0.25 g/l) of pregnant females and drug treatment was maintained through lactation. At 21 days, antibiotic-treated litters were sacrificed, pinna removed, and eardrums inspected through the external auditory canal using a stereomicroscope.

Histology and 3D reconstruction. Mouse heads were fixed using 4% PFA in PBS and paraffin embedded. Longitudinal sections of 5 μm were cut and stained with PAS to examine the middle ear. Sections used for 3D reconstruction were prepared as above except that fixed tissue was embedded in Araldite resins (48). Serial longitudinal sections of 40-μm thickness were stained with epoxy stain (Electron Microscopy Sciences). One digital image of the area including the middle ear cavity to the nasopharynx was taken for each ear of each section. AMIRA software (Mercury Computer Systems) was used to align the stack for each ear, to select and contour each area of interest (middle ear cavity, eustachian tube, and nasopharynx), and to generate a 3D surface view for each ear. Measurements were made from 3D reconstructed images.

Skeletal preparations. Skulls from newborn mice were fixed in 95% ethanol, stained with Alcian blue solution, washed in 95% ethanol, and stained in alizarin red solution (44).

Scanning electronic microscopy. Skulls from 3-week-old and 16-month-old mice were fixed in 1.5% PFA/2.5% glutaraldehyde in 0.1 M phosphate buffer (pH 7.3). To ensure complete fixation, the external auditory canal was flushed with fixative. After decalcification (0.12M EDTA, pH 7), middle ear cavities were dissected and then gradually dehydrated. Samples were subject to the critical drying point process and gold coated prior to observation using scanning electron microscopy (Carl Zeiss SMT). Four ears of each genotype were evaluated.

Statistics. Statistical significance (i.e., *P* values) of group sizes for dichotomous variables was assessed using Fisher's exact test, assuming a 2-tailed distribution. The significance of differences in the means of a quantitative trait was assessed by 2-tailed Student's *t* test. For all tests, $P < 0.05$ was considered significant.

Acknowledgments

We thank Connie Miller, Hoabing Wang, Irfan Saadi, Anne Pizard, Claudio Punzo, and Leslie Liberman for their technical help and advice and friendship. This project was support by grants from the Howard Hughes Medical Institute (to C.E. Seidman), the NIH (to J.G. Seidman and C.E. Seidman), and NIDCD RO1 DC0188 and NIDCD P30 DC 05209 (to M.C. Liberman).

Received for publication June 5, 2007, and accepted in revised form November 28, 2007.

Address correspondence to: J.G. Seidman, Department of Genetics, Harvard Medical School, 77 Avenue Louis Pasteur, Boston, Massachusetts 02115, USA. Phone: (617) 432-7830; Fax: (617) 432-7832; E-mail: seidman@genetics.med.harvard.edu.

Christine E. Seidman and J.G. Seidman contributed equally to this work.

1. Schappert, S.M. 1992. Office visits for otitis media: United States, 1975-90. *Adv. Data.* **214**:1–19.
2. Bondy, J., Berman, S., Glazner, J., and Lezotte, D. 2000. Direct expenditures related to otitis media diagnoses: extrapolations from a pediatric medicaid cohort. *Pediatrics.* **105**:E72.
3. Paradise, J.L., et al. 1997. Otitis media in 2253 Pittsburgh-area infants: prevalence and risk factors during the first two years of life. *Pediatrics.* **99**:318–333.
4. Paradise, J.L., et al. 2003. Otitis media and tympanostomy tube insertion during the first three years of life: developmental outcomes at the age of four years. *Pediatrics.* **112**:265–277.
5. Bluestone, C.D. 2005. *The Eustachian tube: structure, function and role in the middle ear.* B.C. Decker, Inc. Hamilton, Ontario, Canada. 240 pp.
6. Casselbrant, M.L., et al. 1999. The heritability of otitis media: a twin and triplet study. *JAMA.* **282**:2125–2130.
7. Casselbrant, M.L., and Mandel, E.M. 2005. Genetic susceptibility to otitis media. *Curr. Opin. Allergy Clin. Immunol.* **5**:1–4.
8. Online Mendelian Inheritance in Man. http://www.ncbi.nlm.nih.gov/sites/entrez?db=OMIM.
9. Chen, A., et al. 1995. Phenotypic manifestations of branchio-oto-renal syndrome. *Am. J. Med. Genet.* **58**:365–370.
10. Pfister, M., et al. 2002. A 4-bp insertion in the eya-homologous region (eyaHR) of EYA4 causes hearing impairment in a Hungarian family linked to DFNA10. *Mol. Med.* **8**:607–611.
11. Wayne, S., et al. 2001. Mutations in the transcriptional activator EYA4 cause late-onset deafness at the DFNA10 locus. *Hum. Mol. Genet.* **10**:195–200.
12. O'Neill, M.E., et al. 1996. A gene for autosomal dominant late-onset progressive non-syndromic hearing loss, DFNA10, maps to chromosome 6. *Hum. Mol. Genet.* **5**:853–856.
13. Schonberger, J., et al. 2005. Mutation in the transcriptional coactivator EYA4 causes dilated cardiomyopathy and sensorineural hearing loss. *Nat. Genet.* **37**:418–422.
14. De Leenheer, E.M., et al. 2002. DFNA10/EYA4 — the clinical picture. *Adv. Otorhinolaryngol.* **61**:73–78.
15. Ohto, H., et al. 1999. Cooperation of six and eya in activation of their target genes through nuclear translocation of Eya. *Mol. Cell. Biol.* **19**:6815–6824.
16. Borsani, G., et al. 1999. EYA4, a novel vertebrate gene related to Drosophila eyes absent. *Hum. Mol. Genet.* **8**:11–23.
17. Rayapureddi, J.P., et al. 2003. Eyes absent represents a class of protein tyrosine phosphatases. *Nature.* **426**:295–298.
18. Tootle, T.L., et al. 2003. The transcription factor Eyes absent is a protein tyrosine phosphatase. *Nature.* **426**:299–302.
19. Li, X., et al. 2003. Eya protein phosphatase activity regulates Six1-Dach-Eya transcriptional effects in mammalian organogenesis. *Nature.* **426**:247–254.
20. Rebay, I., Silver, S.J., and Tootle, T.L. 2005. New vision from Eyes absent: transcription factors as enzymes. *Trends Genet.* **21**:163–171.
21. Rosowski, J.J., Brinsko, K.M., Tempel, B.I., and Kujawa, S.G. 2003. The aging of the middle ear in 129S6/SvEvTac and CBA/CaJ mice: measure-

ments of umbo velocity, hearing function, and the incidence of pathology. *J. Assoc. Res. Otolaryngol.* **4**:371–383.
22. McGinn, M.D., Bean-Knudsen, D., and Ermel, R.W. 1992. Incidence of otitis media in CBA/J and CBA/CaJ mice. *Hear. Res.* **59**:1–6.
23. Park, K., and Lim, D.J. 1992. Luminal development of the eustachian tube and middle ear: murine model. *Yonsei Med. J.* **33**:159–167.
24. Roberts, D.S., and Miller, S.A. 1998. Apoptosis in cavitation of middle ear space. *Anat. Rec.* **251**:286–289.
25. Girard, D., Finegan, S.M., Dunne, M.W., and Lame, M.E. 2005. Enhanced efficacy of single-dose versus multi-dose azithromycin regimens in preclinical infection models. *J. Antimicrob. Chemother.* **56**:365–371.
26. Kubba, H., Pearson, J.P., and Birchall, J.P. 2000. The aetiology of otitis media with effusion: a review. *Clin. Otolaryngol. Allied Sci.* **25**:181–194.
27. Xu, P.X., et al. 1999. Eya1-deficient mice lack ears and kidneys and show abnormal apoptosis of organ primordia. *Nat. Genet.* **23**:113–117.
28. Mallo, M. 2003. Formation of the outer and middle ear, molecular mechanisms. *Curr Top Dev. Biol.* **57**:85–113.
29. el-Sayed, Y., al-Sarhani, A., and al-Essa, A.R. 1997. Otological manifestations of primary ciliary dyskinesia. *Clin. Otolaryngol. Allied Sci.* **22**:266–270.
30. Zheng, W., et al. 2003. The role of Six1 in mammalian auditory system development. *Development.* **130**:3989–4000.
31. Hardisty, R.E., et al. 2003. The deaf mouse mutant Jeff (Jf) is a single gene model of otitis media. *J. Assoc. Res. Otolaryngol.* **4**:130–138.
32. Hardisty-Hughes, R.E., et al. 2006. A mutation in the F-box gene, Fbxo11, causes otitis media in the Jeff mouse. *Hum. Mol. Genet.* **15**:3273–3279.
33. Piza, J., Northrop, C., and Eavey, R.D. 1998. Embryonic middle ear mesenchyme disappears by redistribution. *Laryngoscope.* **108**:1378–1381.
34. Larsen, P.L., Tos, M., Kuijpers, W., and van der Beek, J.M. 1992. The early stages of polyp formation. *Laryngoscope.* **102**:670–677.
35. Matsune, S., Sando, I., and Takahashi, H. 1992. Distributions of eustachian tube goblet cells and glands in children with and without otitis media. *Ann. Otol. Rhinol. Laryngol.* **101**:750–754.
36. Steel, K.P., Moorjani, P., and Bock, G.R. 1987. Mixed conductive and sensorineural hearing loss in LP/J mice. *Hear. Res.* **28**:227–236.
37. Vogler, C., et al. 2001. A novel model of murine mucopolysaccharidosis type VII due to an intracisternal a particle element transposition into the beta-glucuronidase gene: clinical and pathologic findings. *Pediatr. Res.* **49**:342–348.
38. Liao, J., et al. 2004. Full spectrum of malformations in velo-cardio-facial syndrome/DiGeorge syndrome mouse models by altering Tbx1 dosage. *Hum. Mol. Genet.* **13**:1577–1585.
39. Schmidt-Ullrich, R., et al. 2001. Requirement of NF-kappaB/Rel for the development of hair follicles and other epidermal appendices. *Development.* **128**:3843–3853.
40. Yang, A., et al. 2000. p73-deficient mice have neurological, pheromonal and inflammatory defects but lack spontaneous tumours. *Nature.* **404**:99–103.
41. MacArthur, C.J., Hefeneider, S.H., Kempton, J.B., and Trune, D.R. 2006. C3H/HeJ mouse model for spontaneous chronic otitis media. *Laryngoscope.* **116**:1071–1079.
42. Parkinson, N., et al. 2006. Mutation at the Evi1 locus in Junbo mice causes susceptibility to otitis media. *PLoS Genet.* **2**:e149.
43. Zhang, Y., Buchholz, F., Muyrers, J.P., and Stewart, A.F. 1998. A new logic for DNA engineering using recombination in Escherichia coli. *Nat. Genet.* **20**:123–128.
44. Pizard, A., et al. 2005. Connexin 40, a target of transcription factor Tbx5, patterns wrist, digits, and sternum. *Mol. Cell. Biol.* **25**:5073–5083.
45. Darrow, K.N., Maison, S.F., and Liberman, M.C. 2007. Selective removal of lateral olivocochlear efferents increases vulnerability to acute acoustic injury. *J. Neurophysiol.* **97**:1775–1785.
46. Maison, S.F., et al. 2003. Loss of alpha CGRP reduces sound-evoked activity in the cochlear nerve. *J. Neurophysiol.* **90**:2941–2949.
47. Girard, A.E., et al. 1987. Pharmacokinetic and in vivo studies with azithromycin (CP-62,993), a new macrolide with an extended half-life and excellent tissue distribution. *Antimicrob. Agents. Chemother.* **31**:1948–1954.
48. Hirose, K., and Liberman, M.C. 2003. Lateral wall histopathology and endocochlear potential in the noise-damaged mouse cochlea. *J. Assoc. Res. Otolaryngol.* **4**:339–352.